Developmental Programming: Effect of Prenatal Steroid Excess on Intraovarian Components of Insulin Signaling Pathway and Related Proteins in Sheep[1]

Hugo H. Ortega,[3,4] Florencia Rey,[3,4] Melisa M.L. Velazquez,[3] and Vasantha Padmanabhan[2,5]

Department of Morphological Sciences,[3] Faculty of Veterinary Sciences, National University of Litoral, Esperanza, Santa Fe, Argentina
Argentine National Research Council (CONICET),[4] Buenos Aires, Argentina
Department of Pediatrics and the Reproductive Sciences Program,[5] University of Michigan, Ann Arbor, Michigan

ABSTRACT

Prenatal testosterone (T) excess increases ovarian follicular recruitment, follicular persistence, insulin resistance, and compensatory hyperinsulinemia. Considering the importance of insulin in ovarian physiology, in this study, using prenatal T- and dihydrotestosterone (DHT, a nonaromatizable androgen)-treated female sheep, we tested the hypothesis that prenatal androgen excess alters the intraovarian insulin signaling cascade and metabolic mediators that have an impact on insulin signaling. Changes in ovarian insulin receptor (INSRB), insulin receptor substrate 1 (IRS1), mammalian target of rapamycin (MTOR), phosphatidylinositol 3-kinase (PIK3), peroxisome proliferator-activated receptor-gamma (PPARG), and adiponectin proteins were determined at fetal (Days 90 and 140), postpubertal (10 mo), and adult (21 mo) ages by immunohistochemistry. Results indicated that these proteins were expressed in granulosa, theca, and stromal compartments, with INSRB, IRS1, PPARG, and adiponectin increasing in parallel with advanced follicular differentiation. Importantly, prenatal T excess induced age-specific changes in PPARG and adiponectin expression, with increased PPARG expression evident during fetal life and decreased antral follicular adiponectin expression during adult life. Comparison of developmental changes in prenatal T and DHT-treated females found that the effects on PPARG were programmed by androgenic actions of T, whereas the effects on adiponectin were likely by its estrogenic action. These results suggest a role for PPARG in the programming of ovarian disruptions by prenatal T excess, including a decrease in antral follicular adiponectin expression and a contributory role for adiponectin in follicular persistence and ovulatory failure.

developmental biology, fetal programming, follicular development, insulin, ovary, PCOS, sheep

INTRODUCTION

Ovarian folliculogenesis is a lengthy and intricately regulated process involving precisely orchestrated differentiation of both the somatic and germ cells [1]. Animal models that manifest disrupted folliculogenesis serve as valuable resources for understanding the mechanisms underlying follicular differentiation and ovarian pathologies. For instance, experimental exposure of sheep or monkey fetuses to excess testosterone (T) culminates in ovarian and reproductive phenotypes [2–4] similar to that of women with polycystic ovarian syndrome (PCOS) [5–7], a major infertility disorder. At the ovarian level, prenatal T-treated sheep manifest multifollicular ovarian morphology [8], enhanced follicular recruitment [9], and follicular persistence [10, 11]. Using prenatal T- and dihydrotestosterone (DHT)-treated sheep, we recently found that prenatal T and DHT excess alters androgen receptor (AR) and estrogen receptors (ESR1, ESR2), but not progesterone receptor (PGR-B), protein expression in the ovary, in a developmental time-, steroid-, follicular stage-, and cell-specific manner [12]. These studies provided evidence that multifollicular ovarian morphology [8], follicular persistence [10, 11], and depletion [9] are programmed at least in part via altered AR signaling during fetal development, with subsequent manifestation of ovarian pathology in adulthood facilitated via altered ESR1, ESR2, and AR expression [9, 12].

In addition to disruptions with steroid receptor signaling, because prenatal T-treated sheep also manifest peripheral insulin resistance and compensatory hyperinsulinemia [2, 13], and insulin potentiates ovarian steroidogenesis, follicular development, and granulosa cell proliferation [14–17], it is important to assess the potential contribution from members of insulin signaling pathway to ovarian follicular differentiation. Several studies suggest that alterations in the insulin signaling cascade contribute to ovarian dysfunctions [18–22]. Importantly, hyperinsulinemic status with subsequent amplification of theca cell steroidogenesis is thought to be the primary cause of hyperandrogenism in women with PCOS [23–26]. The importance of members of the insulin signaling pathway in reproduction is also evident from gene-targeting studies. For instance, targeted deletion of IRS1 compromises female fertility [27]. Similarly, granulosa cell-specific deletion of PPARG disrupts follicular rupture [28], causing sterility/subfertility [29].

There are several regulatory checkpoints to consider relative to the role of insulin in mediating ovarian disruptions seen in prenatal T-treated sheep. These include the insulin receptor (INSR), via which insulin initiates its signaling, and insulin receptor substrates (IRS) [30, 31], which serve as docking proteins binding the phosphatidylinositol 3-kinase (PIK3) complex, a key regulatory messenger in insulin signaling. PIK3, via its downstream effector RAC-alpha serine/threonine-protein kinase (AKT, otherwise known as protein kinase B or PKB), activates several signaling molecules, including mammalian target of rapamycin (MTOR), a promoter of protein

TABLE 1.   Antibodies used for immunohistochemistry (IHC) and Western blot (WB).

Antigen	Clone and Source	Dilution IHC	Dilution WB
INSRB	Polyclonal (sc-711, Santa Cruz Biotechnology, Santa Cruz, CA)	1:250	1:400
IRS1	Polyclonal (sc-559, Santa Cruz Biotechnology, Santa Cruz, CA)	1:500	1:800
PIK3	Polyclonal (sc-423, Santa Cruz Biotechnology, Santa Cruz, CA)	1:150	1:400
MTOR	Polyclonal (ab51044, Abcam, Cambridge, MA)	1:250	1:400
PPARG	Polyclonal (ab59256, Abcam, Cambridge, MA)	1:300	1:800
Adiponectin	Polyclonal (ab62551, Abcam, Cambridge, MA)	1:300	1:800

synthesis [30–32]. In addition, insulin, in a ligand-independent manner, also activates the peroxisome proliferator-activated receptor-gamma (PPARG) protein, an orphan nuclear receptor and key regulator of insulin sensitivity and glucose homeostasis. Evidence exits in support of the existence of INSR, IRS1, PIK3, MTOR, and PPARG in the ovary [17, 19, 33–36]. Granulosa cells of preantral follicles express INSR, with expression level increasing with follicle growth [37, 38]. Studies in human have found increased expression of *INSR* mRNA in PCOS patients [39], the reproductive phenotype of which prenatal T-treated sheep recapitulate. Of relevance to hyperandrogenic ovarian pathology seen in prenatal T-treated sheep, activation of PPARG with insulin sensitizers ameliorates hyperandrogenism in women with PCOS [40–42].

Furthermore, in addition to the tight coupling of the reproductive system with energy balance, the close relationship between insulin resistance and adiposity, and the amplification of reproductive pathologies with adiposity in women with PCOS [5] as well as prenatal T-treated sheep [43], adipocyte-derived factors are also important players to be considered. Adiponectin, an adipokine, and its receptors are expressed in rat theca-interstitial cells, oocytes, and granulosa cells [44]. Recent studies also implicate adiponectin in the pathogenesis of PCOS [45–49].

Based on the established relation between insulin and ovarian physiology and the association of insulin with PCOS, we tested the hypothesis that prenatal androgen excess disrupts key members of the intraovarian insulin signaling cascade, and other related proteins implicated in the pathogenesis of PCOS, in a development-specific manner. Prenatal T- and DHT-treated female sheep were studied in parallel to determine whether prenatal T effects were mediated by androgenic programming.

MATERIALS AND METHODS

Breeding and Prenatal Treatment

All procedures used in this study were approved by the Institutional Animal Care and Use Committee of the University of Michigan and were consistent with the National Research Council's Guide for the Care and Use of Laboratory Animals. Adult Suffolk ewes with proven fertility were purchased from local farmers and moved to a nearby farm for breeding; this farm was approved by the Unit for Laboratory Animal Medicine of the University of Michigan and inspected by the USDA. Details of maintenance of breeder ewes, breeding, prenatal T and DHT treatment, and lambing have been previously described [11, 50, 51]. Briefly, pregnant ewes were administered twice-weekly i.m. injections of 100 mg of T propionate (1.2 mg/kg; Sigma-Aldrich Corp., St. Louis, MO) or 100 mg DHT propionate (Steraloids, Inc., Newport, RI) suspended in cottonseed oil (Sigma-Aldrich Corp.) beginning on Fetal Day 30 and continuing until Fetal Day 90. Ovaries obtained from control, prenatal T-, and DHT-treated females on Fetal Day 90 (six control fetuses from six dams, six T-treated fetuses from six dams, and six DHT-treated fetuses from five dams), Fetal Day 140 (six control fetuses from five dams, seven T-treated fetuses from seven dams, and five DHT-treated fetuses from five dams), 10 mo of age (five control animals from five dams, six T-treated animals from six dams, and five DHT-treated animals from five dams), and 21 mo of age (five control animals from five dams, eight T-treated animals from eight dams) were used in this study. There were insufficient DHT-treated females born to include

a 21-mo-old prenatal DHT-treated group. Ovaries from 10- and 21-mo-old sheep were collected during the presumptive follicular phase after administration of prostaglandin F2α. Details of euthanasia, ovarian collection, and processing have been published [9, 12]. Paraffin-embedded sections from one ovary from each animal were used in this study. Developmental changes in ovarian follicular distribution determined by ovarian morphometry [9] and changes in steroid receptor expression patterns as determined by immunohistochemistry from the same set of animals have been previously published [12].

Western Blotting

To test the specificity of the primary antibodies used in this study (Table 1), ovaries from adult sheep procured from a local abattoir were homogenized in a radio-immunoprecipitation assay lysis buffer consisting of 1% (v/v) IGEPAL CA630 (octylphenyl-polyethylene glycol), 0.5% (w/v) sodium deoxycholate, 0.1% (w/v) SDS, 1 mM ethylenediaminetetraacetic acid, 50 mM sodium fluoride (all from Sigma-Aldrich Corp.), 0.1 M PBS, and a protease inhibitor cocktail (Complete Mini Protease Inhibitor Cocktail Tablets; Roche, Mannheim, Germany). Ovarian homogenates were centrifuged at $12\,000 \times g$ for 20 min, and the protein concentration in the supernatants was estimated using fluorescence methods (Qubit; Invitrogen, Carlsbad, CA). Sixty μg of protein, along with prestained molecular weight markers (Bio-Rad, Hercules, CA), were separated in SDS-PAGE containing an acrylamide gradient from 4% to 8% (w/v) polyacrylamide for IRS1 and MTOR or from 10% to 15% for INSRB, PIK3, PPARG, and adiponectin according to a procedure previously described [12]. After blotting on nitrocellulose membranes (Hybond ECL Nitrocellulose Membrane; GE Healthcare, Buckinghamshire, U.K.), the membranes were blocked with Tris-buffered saline containing 0.05% (v/v) Tween 20 (Sigma-Aldrich Corp.) and 2% (w/v) nonfat milk and then incubated overnight at 4°C with specific primary antibodies. Bound antibody was detected using anti-rabbit IgG peroxidase antibody (1:500; Amersham, Buckinghamshire, U.K.) and ECL plus Western blotting detection reagents (GE Healthcare).

Immunohistochemistry

For immunohistochemistry, the streptavidin-biotin immunoperoxidase method was employed as described previously [12]. Briefly, the sections were deparaffinized, and antigen retrieval was performed by heating in a microwave. Endogenous peroxidase activity was blocked with 3% H_2O_2 in methanol, and nonspecific binding was blocked with 10% (v/v) normal goat serum. Sections were incubated with primary antibodies (Table 1) for 18 h at 4°C and then with a biotinylated secondary antibody (1:150; goat anti-rabbit IgG, F(ab′)2-B, Biotin conjugated, sc-3840; Santa Cruz Biotechnology, Santa Cruz, CA) for 30 min at room temperature. Detection was by a streptavidin-peroxidase solution (BioGenex, San Ramon, CA), with 3,3-diaminobenzidine (DAB; Dako, Carpinteria, CA) as chromogen. The sections were then counterstained with Mayer hematoxylin, dehydrated, and mounted. Blocking of the endogenous peroxidase activity was confirmed by incubating some sections with DAB alone, and the specificity of the secondary antibodies was tested by replacing the primary antibodies with nonimmune serum. For INSRB and IRS1, an additional control was performed by pre-incubating the primary antibody with an excess of the peptide (for others, peptide was not commercially available) with which it was raised. Because multiple series of histological processing were involved, serial sections of a nonexperimental set of sheep ovaries were included with each series to allow normalization across series. Each immunohistochemical series included randomly selected slides with ovarian sections from different ages and treatments. Follicle classes were distinguished using criteria previously established [12] and included primordial, primary, small preantral, large preantral, and antral follicles.

Image Analysis

Details of image analysis have been described previously [12, 52]. Briefly, for each marker, to avoid the possibility of follicular overlap, two
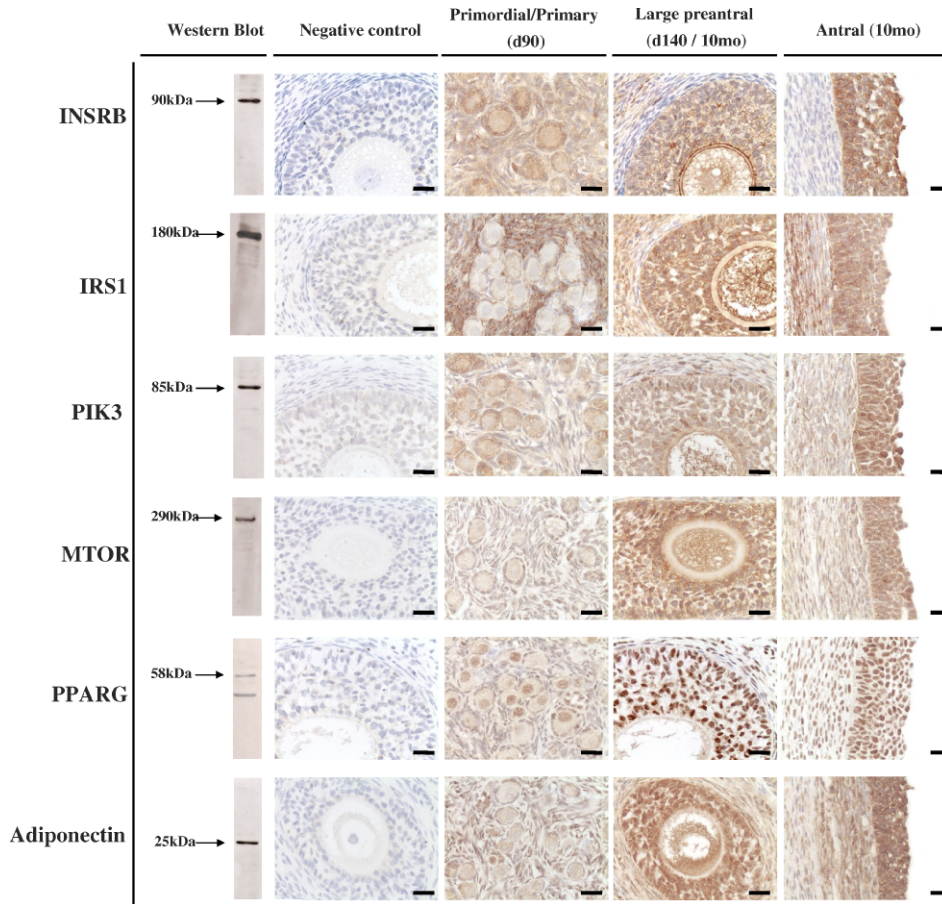
FIG. 1. Representative images of INSRB, IRS1, PIK3, MTOR, PPARG, and adiponectin immunostaining in primordial/primary (Fetal Day 90), large preantral (Fetal Day 140/10-mo-old), and antral (10-mo-old) follicles are shown in the right three panels. Verification of antibody specificity by Western blot analyses of ovarian homogenate and negative controls for immunostaining demonstrating the specificity of the antibody are shown in the left two panels, respectively. Bar = 25μm.

sections (the first third into the ovary and the second two thirds into the ovary) were used for immunohistochemical quantification. All growing follicles in both sections were analyzed (ranged between 8 and 15 for each follicular class). For primordial follicles, the slides were scanned left to right from the top, and the first 20 primordial follicles that were distinct and showed no overlap with neighboring follicles were used. Only healthy follicles without atretic signs (pycnotic nucleus and loss of cell adhesion in the granulosa layer) were evaluated, and to avoid subjectivity and differences in location of proteins, all the analyzed images covered granulosa from antrum to theca. Also, for each ovary, 10 images of stromal tissue were analyzed in the center of the ovary.

The image analysis performed using the Image Pro-Plus 3.0.1 system (Media Cybernetics, Silver Spring, MA) was described previously [12]. Images were digitized with an Olympus C5060 digital camera mounted on a conventional light microscope (Olympus BH-2; Olympus Co., Tokyo, Japan). The average density (percentage of immunopositive area) for each antibody reaction was calculated as a percentage of total area evaluated through color segmentation analysis, which extracts objects by locating all objects of a specific color (brown stain). These values were verified and normalized, with the controls carried across various runs using the same region (verified by image comparison) for calibration. The percentage of immunopositive area was calculated separately for each follicular compartment (granulosa, theca interna, and theca externa) and stroma. Sections were analyzed with the observer blinded to treatment. Since the immunostaining and image analyses are optimized for each protein, quantitative comparisons across proteins were not possible. The major strength of the well-validated imaging approach used in this study is the visualization of in situ localization of proteins within cells of interest. Quantification of biological markers using this approach has been successfully applied to quantify immunoreactivity in different tissues [12, 53]. Antigen expression in tissue sections can be expressed as either mean staining intensity or fraction of the stained area (average density [percentage of immunopositive area]). While mean staining intensity measurements show changes in relative antigen expression when they are ubiquitously expressed and equally distributed in compartments of interest, in scenarios where differences in cellular distributions are unknown the average density is more useful [54, 55]. This type of densitometrical methodology has been previously

validated by biochemical methods of protein induction and quantification [56].

Statistical Analyses

The average density (percentage of immunopositive area) of each follicular compartment (granulosa and theca) within a follicle class was first averaged, and then a group mean across follicles was derived for each follicle type within an animal. When more than one fetus was studied per dam, the data were averaged before analyses. A statistical software package (SPSS 11.0 for Windows; SPSS, Inc., Chicago, IL) was used for performing the statistical tests. Data were compared by ANOVAs, followed by Duncan multiple range tests. A $P < 0.05$ value was considered significant. Results are expressed as mean ± SEM.

RESULTS

Antibody Specificity

Western blot recognition of proteins in ovarian homogenate and immunohistochemical localization of the six proteins in ovarian sections are summarized in Figure 1. Western blot analysis revealed positive bands of appropriate sizes for each of the proteins studied (Fig. 1, left). The INSRB, IRS1, PIK3, MTOR, and adiponectin antibodies detected a single band at 90, 180, 85, 290, and 25 kDa, respectively, whereas two bands around 58 kDa were observed for PPARG. No specific bands were detected after incubating sections in the absence of the primary antibodies (Fig. 1, negative control) or preincubating the primary antibody with an excess of the peptide with which it was raised (when commercially available; INSRB and IRS1; not shown). Specific cytoplasmic staining was detected for all proteins except PPARG, which showed

FIG. 2. Relative expression (measured as percentage of immunopositive area) of INSRB, IRS1, PIK3, MTOR, PPARG, and adiponectin in ovaries of control Day 90 and Day 140 fetuses and 10- and 21-mo-old sheep in control. Significant differences across follicle classes are shown by differing letters. Significant differences within follicular compartments across ages are indicated by asterisks; *$P < 0.05$, **$P < 0.01$.
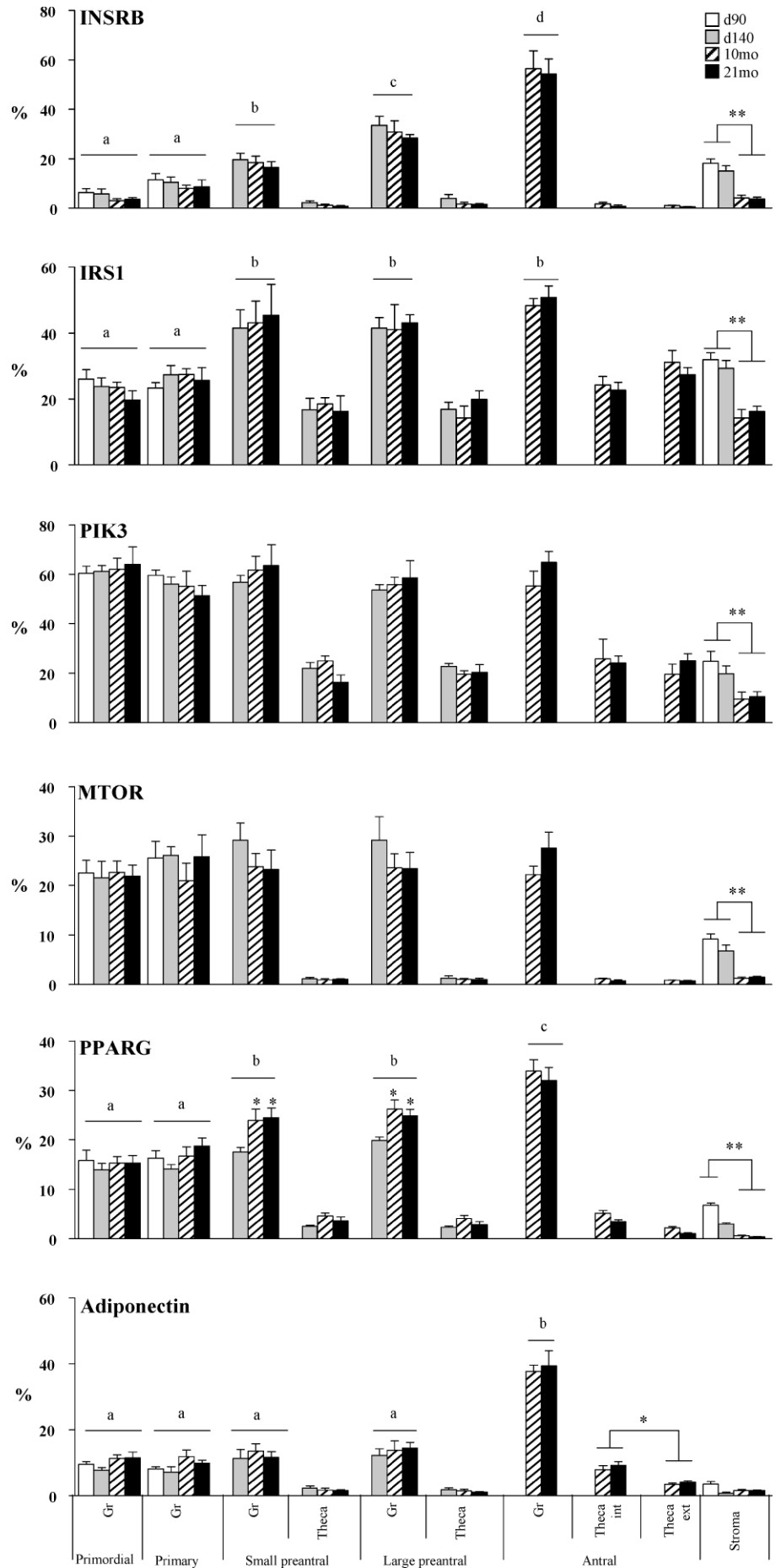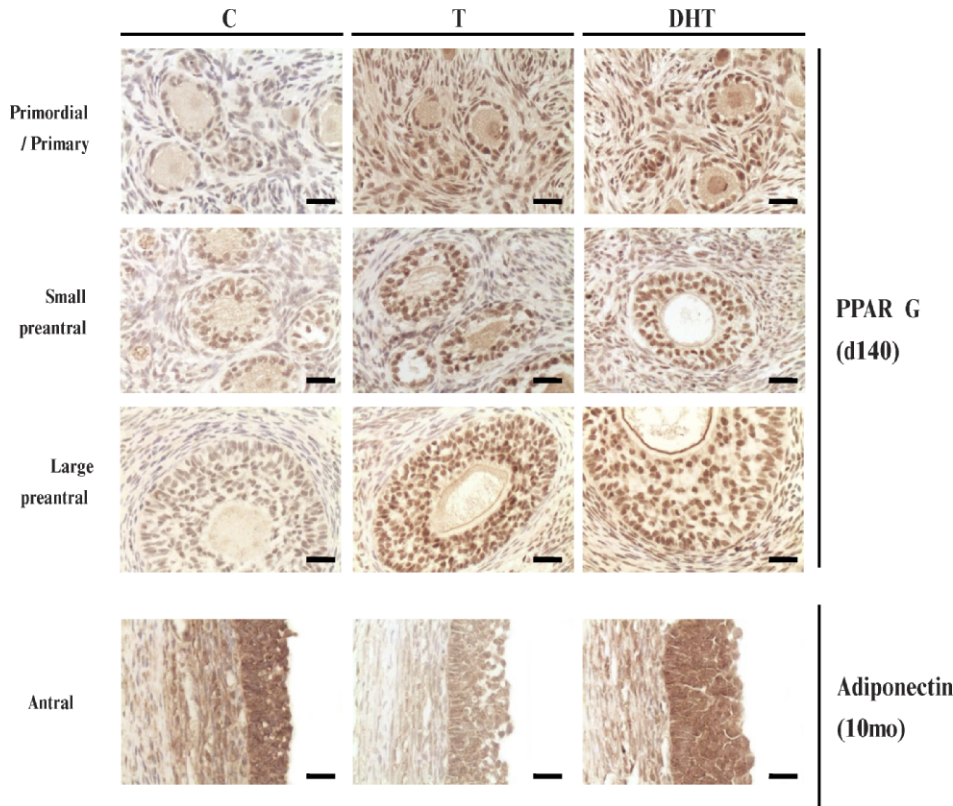
FIG. 3. Representative images of PPARG immunostaining in primordial/primary, small, and large preantral follicles (Fetal Day 90) and adiponectin immunostaining in antral follicles (10-mo-old) of control, prenatal T-treated, and DHT-treated sheep. Bar = 25 μm.

nuclear staining in the ovaries (Fig. 1, right three vertical panels).

Age-Related Changes in Ovarian Expression of INSRB, IRS1, PIK3, MTOR, PPARG, and Adiponectin

Representative patterns of immunostaining of key markers of insulin signaling pathway in primordial/primary (from Fetal Day 90), preantral (from Fetal Day 140 or postpubertal 10-mo-old), and antral follicles (10-mo-old) from control females are shown in Figure 1, and a quantitative analysis of the expression of these proteins from immunohistochemical analyses is shown in Figure 2 and Table 2. INSRB was localized in the cytoplasm of granulosa and stromal cells, while thecal cells showed a weak immunostaining. With the increase in the size of the follicles, the immunostaining in the granulosa cell compartment increased significantly ($P < 0.01$; Fig. 2). IRS1 was detected in the cytoplasm of granulosa, thecal, and stromal cells, with a significantly higher expression in granulosa of preantral and antral follicles compared with primordial/primary follicles ($P < 0.01$). No differences were evident across ages in the thecal compartment. Expression levels of INSR and IRS1 were both higher in stroma of Day 90 and Day 140 fetuses compared to those of 10- or 21-mo-old females ($P < 0.01$).

PIK3 was also highly expressed in the cytoplasm of granulosa, with less immunostaining in thecal and stromal cells (Fig. 1). No difference in level of expression was evident across follicular stages (Fig. 2). Expression levels of PIK3, similar to INSRB and IRS1, were higher in the stroma of fetal animals compared to those of 10- or 21-mo-old animals ($P < 0.01$; Fig. 2). Expression of MTOR protein was high in the cytoplasm of granulosa cells and did not differ across follicular stages (Figs. 1 and 2). Expression of MTOR staining was comparatively weak in thecal and stromal cells, although the expression level in the stroma of fetal animals was higher relative to that of 10- or 21-mo-old animals ($P < 0.01$; Fig. 2).

Compared to other proteins discussed above, PPARG was the only protein localized in the nucleus with predominant expression in granulosa cells (Fig. 1). Expression levels of PPARG increased significantly as the size of follicles increased ($P < 0.01$; Fig. 2). PPARG immunostaining was lower in theca cells. Similar to all other proteins discussed above, the expression level of PPARG in stromal cells was higher in fetal ovaries compared to ovaries from 10- or 21-mo-old animals ($P < 0.01$). In granulosa of preantral follicles, the expression level of PPARG in Day 140 fetuses was lower than that of 10- or 21-mo-old animals ($P < 0.05$).

Higher expression of adiponectin was evident in granulosa cells relative to other cell types. Adiponectin immunostaining was higher in granulosa cells of antral follicles compared to other follicular types ($P < 0.01$). Compared to granulosa cells, the level of immunostaining was lower in thecal cells, with expression showing a tendency to be higher in antral follicles than in other follicular types ($P = 0.06$). Expression level was also higher in theca interna than theca externa ($P < 0.05$). Adiponectin expression was also lower in the stroma and in contrast to all other markers studied, did not show age-specific changes.

Effects of Prenatal T and DHT Treatment

Prenatal T or DHT treatment had no effect on INSRB, IRS1, PIK3, and MTOR protein expression in any of the cellular compartments at any fetal or postpubertal age studied (Table 2). In contrast, prenatal T and DHT treatment increased ($P < 0.05$) PPARG expression in Fetal Day 90 stromal cells (Figs. 3 and 4 and Table 2). Prenatal DHT but not T increased PPARG expression in granulosa cells of primordial and primary follicles of Fetal Day 90 ovaries (Figs. 3 and 4 and Table 2). Prenatal T treatment increased PPARG immunostaining ($P < 0.05$) in granulosa cells of primary as well as small and large preantral follicles and in thecal cells of large preantral and

TABLE 2. Relative expression (measured as a percentage of immunopositive area) of INSRB, IRS1, PIK3, MTOR, PPARG, and adiponectin in ovaries procured from Day 90 (D90) and Day 140 (D140) fetuses and 10-mo-old (10mo) and 21-mo-old (21mo) control (C), prenatal T, and DHT-treated sheep.[a]

Age	Treatment	Primordial Gr	Primary Gr	Small preantral Gr	Small preantral Theca	Large preantral Gr	Large preantral Theca	Antral Gr	Antral Theca interna	Antral Theca externa	Stroma
INSRB[b]											
D90	C	6.28 ± 1.61	11.58 ± 2.50								18.17 ± 1.78
D90	T	5.14 ± 1.04	9.54 ± 1.78								17.08 ± 2.08
D90	DHT	6.62 ± 0.92	11.31 ± 2.19								20.76 ± 2.11
D140	C	5.85 ± 1.91	10.40 ± 2.26	19.69 ± 2.51	2.10 ± 0.87	33.54 ± 3.62	3.96 ± 1.53				15.12 ± 2.09
D140	T	6.96 ± 1.42	10.97 ± 1.38	22.15 ± 6.01	3.23 ± 1.45	32.46 ± 5.17	2.34 ± 0.45				14.43 ± 1.72
D140	DHT	6.45 ± 1.24	8.02 ± 1.06	19.16 ± 3.55	2.61 ± 1.24	37.28 ± 7.48	3.67 ± 0.92				15.21 ± 0.96
10mo	C	3.09 ± 0.73	8.07 ± 1.15	18.54 ± 2.56	1.15 ± 0.44	30.77 ± 4.56	1.65 ± 0.67	56.47 ± 7.15	1.73 ± 0.61	0.98 ± 0.26	4.11 ± 1.15
10mo	T	2.96 ± 0.85	8.37 ± 0.85	19.33 ± 1.03	1.33 ± 0.48	32.05 ± 1.66	1.29 ± 0.34	64.81 ± 3.92	2.32 ± 0.58	1.11 ± 0.32	4.34 ± 0.62
10mo	DHT	2.31 ± 0.43	7.86 ± 0.58	19.91 ± 1.04	1.60 ± 0.40	25.97 ± 3.43	1.88 ± 0.58	59.17 ± 6.27	2.00 ± 1.01	1.01 ± 061	4.51 ± 067
21mo	C	3.60 ± 0.69	8.54 ± 2.89	16.47 ± 2.42	0.80 ± 0.26	28.42 ± 1.34	1.49 ± 0.32	54.28 ± 6.05	0.80 ± 0.50	0.47 ± 0.26	3.63 ± 0.82
21mo	T	2.15 ± 0.39	9.23 ± 1.28	17.81 ± 2.62	1.36 ± 0.24	31.08 ± 2.24	1.68 ± 0.35	59.74 ± 2.69	1.07 ± 0.56	0.79 ± 0.31	3.46 ± 0.71
IRS1[c]											
D90	C	26.05 ± 2.85	23.31 ± 1.67								31.86 ± 2.20
D90	T	26.25 ± 1.63	21.94 ± 2.20								30.94 ± 3.98
D90	DHT	24.57 ± 1.91	22.02 ± 1.42								30.00 ± 1.72
D140	C	23.83 ± 2.54	27.28 ± 2.83	41.58 ± 5.44	16.78 ± 3.50	41.52 ± 3.18	16.92 ± 2.11				29.26 ± 2.38
D140	T	24.05 ± 2.70	25.69 ± 2.03	45.90 ± 4.80	18.19 ± 2.74	43.92 ± 2.38	15.06 ± 1.58				27.42 ± 2.52
D140	DHT	25.20 ± 2.80	22.36 ± 2.75	46.72 ± 4.72	21.70 ± 3.44	39.29 ± 3.13	15.88 ± 2.13				29.45 ± 2.24
10mo	C	23.50 ± 1.60	27.43 ± 1.69	43.13 ± 6.58	18.54 ± 1.86	41.05 ± 7.60	14.24 ± 3.64	48.31 ± 2.08	24.25 ± 2.62	31.05 ± 3.69	14.28 ± 2.58
10mo	T	24.63 ± 3.48	25.33 ± 1.83	47.99 ± 4.34	20.37 ± 1.74	44.04 ± 5.73	16.80 ± 4.45	51.27 ± 6.12	23.15 ± 2.37	32.29 ± 2.64	17.64 ± 1.49
10mo	DHT	22.28 ± 1.50	25.43 ± 1.69	44.07 ± 2.57	21.31 ± 2.64	42.07 ± 4.80	21.08 ± 3.87	49.08 ± 5.61	19.95 ± 2.72	28.61 ± 2.26	15.55 ± 1.62
21mo	C	19.69 ± 2.76	25.63 ± 3.85	45.38 ± 9.39	16.27 ± 4.69	43.10 ± 2.48	19.88 ± 2.60	50.77 ± 3.50	22.64 ± 2.40	27.28 ± 2.22	16.18 ± 1.62
21mo	T	22.92 ± 2.23	24.19 ± 2.96	41.30 ± 4.18	18.10 ± 2.39	45.93 ± 3.27	23.50 ± 2.27	54.09 ± 2.98	24.03 ± 2.22	30.10 ± 2.46	18.98 ± 1.08
PIK3[d]											
D90	C	60.46 ± 2.87	59.65 ± 1.96								24.87 ± 3.99
D90	T	57.63 ± 1.93	58.73 ± 2.19								22.19 ± 3.42
D90	DHT	57.32 ± 1.22	55.28 ± 2.73								21.27 ± 1.76
D140	C	61.13 ± 2.33	56.02 ± 2.88	56.90 ± 2.70	21.97 ± 2.31	53.59 ± 2.27	22.75 ± 1.23				19.86 ± 3.13
D140	T	61.95 ± 1.98	54.47 ± 3.15	58.67 ± 1.89	23.60 ± 1.50	54.32 ± 1.55	24.36 ± 1.64				20.62 ± 1.66
D140	DHT	57.01 ± 3.95	56.32 ± 2.71	59.24 ± 3.55	24.71 ± 2.68	59.88 ± 2.03	23.27 ± 1.68				19.59 ± 2.77
10mo	C	62.01 ± 4.48	55.10 ± 6.09	61.76 ± 5.45	25.00 ± 1.97	55.78 ± 3.01	19.68 ± 1.34	55.31 ± 5.95	25.85 ± 7.94	19.52 ± 4.14	9.56 ± 2.92
10mo	T	58.22 ± 3.13	59.21 ± 5.96	65.07 ± 5.80	26.07 ± 1.62	48.91 ± 4.01	20.32 ± 3.45	60.79 ± 9.81	23.65 ± 3.09	15.98 ± 3.36	8.19 ± 2.39
10mo	DHT	64.00 ± 4.33	52.66 ± 4.46	59.00 ± 3.65	24.45 ± 1.71	51.94 ± 4.17	24.78 ± 3.33	63.37 ± 7.23	20.24 ± 3.17	16.29 ± 2.11	8.02 ± 2.41
21mo	C	64.00 ± 7.01	51.41 ± 4.13	63.49 ± 8.49	16.37 ± 2.94	58.49 ± 6.95	20.42 ± 3.02	64.72 ± 4.52	24.11 ± 2.84	25.04 ± 2.85	10.66 ± 1.89
21mo	T	68.55 ± 5.95	53.44 ± 5.21	59.76 ± 6.39	18.50 ± 3.76	56.03 ± 5.85	16.76 ± 2.70	61.68 ± 7.51	27.66 ± 3.56	26.03 ± 4.49	9.73 ± 1.94
MTOR[e]											
D90	C	22.59 ± 2.55	25.59 ± 3.36								9.23 ± 1.01
D90	T	18.57 ± 1.46	19.12 ± 3.11								6.80 ± 1.06
D90	DHT	20.64 ± 1.35	22.79 ± 2.46								6.12 ± 1.66
D140	C	21.57 ± 3.34	26.14 ± 1.67	29.17 ± 3.46	1.14 ± 0.32	29.15 ± 4.79	1.28 ± 0.47				6.85 ± 1.14
D140	T	24.20 ± 2.38	26.77 ± 3.29	28.07 ± 3.95	1.41 ± 0.35	29.43 ± 1.47	1.22 ± 0.32				5.63 ± 0.92
D140	DHT	18.78 ± 2.90	22.44 ± 1.92	27.46 ± 1.77	0.63 ± 0.23	23.98 ± 3.04	1.03 ± 0.38				7.71 ± 1.48
10mo	C	22.72 ± 2.26	20.96 ± 3.61	23.87 ± 2.66	0.93 ± 0.20	23.60 ± 2.80	1.06 ± 0.16	22.19 ± 1.74	1.12 ± 0.13	0.82 ± 0.09	1.25 ± 0.22
10mo	T	23.10 ± 2.78	22.43 ± 2.32	25.04 ± 3.58	1.02 ± 0.19	26.12 ± 2.43	1.20 ± 0.13	23.06 ± 2.22	1.27 ± 0.20	0.76 ± 0.12	1.02 ± 0.17
10mo	DHT	18.54 ± 4.91	20.70 ± 3.47	27.68 ± 1.64	0.83 ± 0.13	26.83 ± 2.50	1.24 ± 0.23	25.02 ± 1.77	1.05 ± 0.13	0.70 ± 0.10	1.48 ± 0.45
21mo	C	21.93 ± 2.23	25.88 ± 4.36	23.30 ± 3.87	1.04 ± 0.10	23.47 ± 3.22	0.98 ± 0.31	27.58 ± 3.19	0.68 ± 0.27	0.71 ± 0.13	1.51 ± 0.18
21mo	T	24.37 ± 1.97	21.21 ± 0.88	26.35 ± 2.12	0.75 ± 0.21	26.65 ± 1.82	1.06 ± 0.16	29.27 ± 0.92	0.92 ± 0.11	1.08 ± 0.11	1.74 ± 0.15

TABLE 2. *Continued.*

Age	Treatment	Primordial Gr	Primary Gr	Small preantral Gr	Small preantral Theca	Large preantral Gr	Large preantral Theca	Antral Gr	Antral Theca interna	Antral Theca externa	Stroma
PPARG[f]											
D90	C	15.81 ± 2.11	16.29 ± 1.53								6.79 ± 0.46
D90	T	19.80 ± 0.74	20.96 ± 2.28								10.56 ± 0.37
D90	DHT	21.72 ± 1.20	22.53 ± 1.83								11.53 ± 0.84
D140	C	13.91 ± 1.27	14.08 ± 0.88	17.53 ± 0.93	2.50 ± 0.23	19.84 ± 0.70	2.34 ± 0.23				2.94 ± 0.24
D140	T	18.00 ± 1.80	21.16 ± 1.82	23.25 ± 0.88	4.72 ± 0.40	24.20 ± 0.69	4.69 ± 0.56				5.39 ± 0.51
D140	DHT	16.75 ± 3.01	22.62 ± 1.22	24.92 ± 0.91	5.57 ± 1.22	25.88 ± 0.81	4.08 ± 0.30				5.26 ± 0.67
10mo	C	15.28 ± 1.34	16.72 ± 1.89	23.93 ± 2.32	4.62 ± 0.60	26.20 ± 1.86	4.12 ± 0.62	33.90 ± 2.31	5.18 ± 0.60	2.19 ± 0.28	0.62 ± 0.14
10mo	T	16.08 ± 1.46	18.96 ± 3.12	21.65 ± 1.35	4.37 ± 0.57	27.72 ± 0.85	3.87 ± 0.45	34.11 ± 2.49	4.52 ± 0.43	2.42 ± 0.45	0.84 ± 0.14
10mo	DHT	18.11 ± 0.91	17.25 ± 1.29	20.61 ± 2.20	4.99 ± 0.32	28.25 ± 1.31	4.38 ± 0.60	32.12 ± 1.89	4.77 ± 0.49	1.87 ± 0.41	0.69 ± 0.13
21mo	C	15.29 ± 1.53	18.73 ± 1.64	24.53 ± 1.93	3.66 ± 0.80	24.90 ± 1.28	2.83 ± 0.66	32.03 ± 2.62	3.47 ± 0.40	1.04 ± 0.18	0.36 ± 0.14
21mo	T	16.57 ± 1.04	17.39 ± 2.16	27.03 ± 0.62	2.91 ± 0.70	28.29 ± 1.02	3.49 ± 0.43	33.06 ± 1.51	3.97 ± 0.69	0.98 ± 0.11	0.44 ± 0.12
Adiponectin[g]											
D90	C	9.53 ± 0.84	8.14 ± 0.70								3.59 ± 0.74
D90	T	10.34 ± 0.92	9.07 ± 0.85								3.91 ± 0.77
D90	DHT	11.12 ± 1.32	7.65 ± 1.17								2.62 ± 0.48
D140	C	7.72 ± 0.88	7.21 ± 1.66	11.36 ± 2.68	2.31 ± 0.61	12.27 ± 1.99	1.79 ± 0.56				0.83 ± 0.23
D140	T	8.64 ± 1.32	6.16 ± 0.81	11.05 ± 1.75	2.06 ± 0.39	10.48 ± 1.00	1.29 ± 0.40				1.24 ± 0.24
D140	DHT	7.95 ± 0.74	7.30 ± 0.37	12.85 ± 2.80	2.23 ± 0.41	12.40 ± 1.92	1.13 ± 0.27				1.04 ± 0.16
10mo	C	11.39 ± 1.04	11.88 ± 2.04	13.57 ± 2.27	1.72 ± 0.58	19.82 ± 2.81	1.52 ± 0.46	37.76 ± 1.86	7.96 ± 1.18	3.46 ± 0.40	1.53 ± 0.35
10mo	T	9.43 ± 1.32	8.78 ± 1.38	10.67 ± 1.67	0.67 ± 0.22	12.10 ± 1.99	1.42 ± 0.67	21.21 ± 0.87	6.67 ± 1.13	1.56 ± 0.32	0.19 ± 0.09
10mo	DHT	13.27 ± 1.84	9.22 ± 1.47	12.86 ± 2.04	0.88 ± 0.13	15.23 ± 1.53	1.31 ± 0.26	31.00 ± 3.49	7.43 ± 0.35	2.21 ± 0.52	0.65 ± 0.17
21mo	C	11.55 ± 1.74	9.91 ± 0.85	11.65 ± 1.81	1.62 ± 0.21	14.52 ± 1.71	1.13 ± 0.16	44.45 ± 4.58	9.28 ± 1.08	4.14 ± 0.41	1.59 ± 0.18
21mo	T	9.53 ± 1.12	8.63 ± 0.83	11.18 ± 1.25	1.26 ± 0.22	10.21 ± 0.92	0.92 ± 0.13	22.52 ± 2.57	7.37 ± 1.04	1.63 ± 0.20	0.72 ± 0.10

a Values are means ± SEM. For each ovarian compartment [granulosa (gr), theca and stromal], follicle stage, age and treatment (trt) are main effects tested.

b Significant main effect and interactions are Gr: follicle stage and stroma: age.

c Significant main effect and interactions are Gr: follicle stage and stroma: age.

d Significant main effect and interactions are stroma: age.

e Significant main effect and interactions are stroma: age.

f Significant main effect and interactions are Gr: follicle stage, age, age × trt; theca: trt, age × trt; stroma: age, trt.

g Significant main effect and interactions are Gr: follicle stage, trt, age × trt; theca: trt; stroma: trt.

FIG. 4. Relative expression (measured as percentage of immunopositive area) of PPARG in ovaries of control, prenatal T-treated, and prenatal DHT-treated Day 90 (d90) and Day 140 (d140) fetuses. For each cellular compartment within each follicle type, bars with * are significantly different from control ($P < 0.05$).
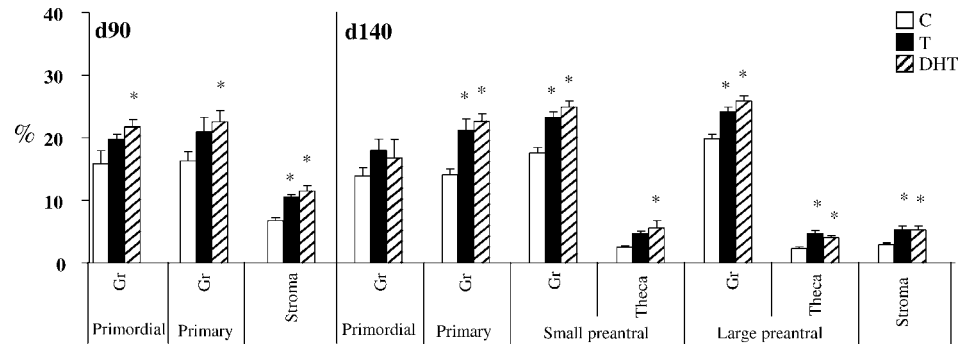
stromal cells of Fetal Day 140 ovaries (Figs. 3 and 4 and Table 2). Effects of prenatal DHT treatment paralleled that of T except that an increase in thecal expression was also evident in small preantral follicles (Figs. 3 and 4 and Table 2). Prenatal T or DHT treatment had no effect on any ovarian compartment in PPARG expression of 10- and 21-mo-old animals (Table 2).

Effects of prenatal T and DHT treatment on adiponectin were diametrically opposite and were evident in ovaries of 10- and 21-mo-old animals but not during fetal life (Figs. 3 and 5 and Table 2). In 10-mo-old animals, prenatal T but not DHT excess reduced adiponectin expression in granulosa cells of large preantral and antral follicles and in theca externa of antral follicles ($P < 0.05$). In contrast, both prenatal T and DHT excess reduced adiponectin immunostaining in the stroma (Figs. 3 and 5 and Table 2; $P < 0.05$). At 21 mo of age (comparison is only between control and prenatal T, as an insufficient number of prenatal DHT females was born for inclusion in this group), effects of prenatal T excess paralleled that seen in 10-mo-old animals, with prenatal T excess decreasing adiponectin immunostaining in granulosa cells of large preantral and antral follicles, theca externa of antral follicles, and stroma (Fig. 5 and Table 2; $P < 0.05$).

DISCUSSION

The findings from this study provide evidence in support of age- and ovarian compartment-specific regulation in the expression and localization of various members of insulin signaling pathway and related proteins in sheep and their modulation by prenatal steroid excess. All proteins studied are expressed in granulosa, theca, and stromal compartments, with many of them (INSRB, IRS1, PPARG, and adiponectin) increasing in parallel with advanced follicular differentiation. Importantly, prenatal T excess induced age-specific changes in PPARG and adiponectin expression, with effects on PPARG evident during fetal life and those of adiponectin evident during adult life. Furthermore, comparative assessment of developmental changes in prenatal T- and DHT-treated females found that the effects on PPARG were programmed by androgenic

actions of T, whereas the effects on granulosa cell expression of adiponectin were likely programmed by its estrogenic action.

Developmental Changes

The increase in granulosa cell expression of INSRB immunostaining with advanced follicular differentiation evidenced in this study parallels increases found in other species [16]. The higher expression seen in large preantral and antral follicles is consistent with a role for insulin in augmenting responsiveness to gonadotropins [19, 39]. The progressive increase in INSRB protein with advanced follicular development was also accompanied by parallel increases in mediators of insulin action, namely IRS1 and PPARG.

Lack of change in PIK3, a key regulatory messenger in insulin signaling, across follicular developmental progression in the face of changes in downstream members of insulin signaling pathway suggests that changes in PIK3 are manifested more at the activity level than the absolute amount per se. Lack of availability of phospho-specific PIK3 and AKT antibodies for immunohistochemical studies in sheep precluded such measures being undertaken. Irrespective of this limitation, changes in downstream regulators of PIK3 and AKT indicate that changes in the activity of these key regulators must have occurred. Inhibition of PIK3 function has been found to block FSH-induced up-regulation/activation of several follicular differentiation markers and signaling proteins that control mRNA translation [57].

Increased expression of PPARG in granulosa cells with increasing follicular differentiation is in agreement with parallel increases seen in the granulosa cells of growing follicles in the rat [58] and is supportive of a role for PPARG in follicular development. The antral follicle-specific increase in adiponectin is also consistent with developmental maturation of the follicle to the preovulatory state. Adiponectin and its receptors are expressed in the ovaries of several mammals [44, 59]. Adiponectin has been found to induce changes in expression of genes/proteins consistent with those that occur during differentiation of the preovulatory follicle [18].

FIG. 5. Relative expression of adiponectin in the ovaries of 10-mo-old (10mo) and 21-mo-old (21mo) control, prenatal T-treated, and prenatal DHT-treated females. For each cellular compartment within each follicle type, bars with * are significantly different from control ($P < 0.05$).
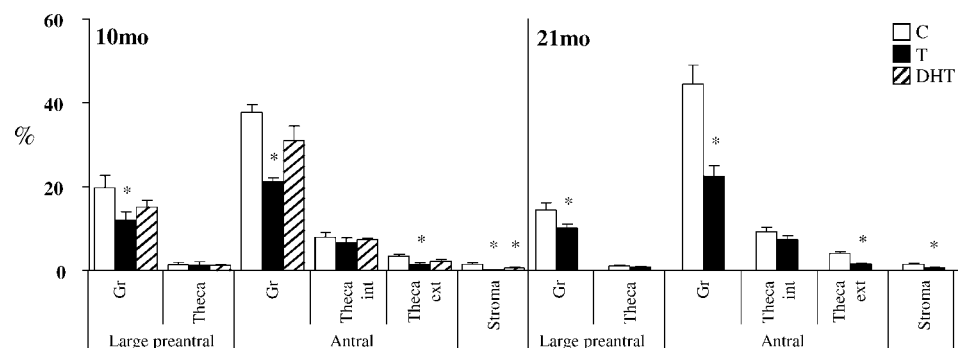
Adiponectin also increases the synthesis of progesterone and estrogen in an additive manner with gonadotropins [59]. Adiponectin also participates in the actions of PPARG [18, 60, 61] by decreasing *LHR* mRNA and insulin-induced androstenedione production in theca cells [62]. The finding that mice lacking adiponectin [63] or adiponectin receptors (ADIPOR1 and/or ADIPOR2) [64] are fertile suggests that adiponectin plays more of a facilitatory role than an obligatory one.

Overall, changes in the expression patterns of members of insulin signaling pathway and related proteins at different stages of follicular development were follicle-specific but independent of age of animals. An exception to this rule was PPARG, with expression of PPARG being higher in preantral follicles obtained from 10- and 21-mo-old animals compared to that of Day 140 fetuses. In contrast, the expression pattern of most of these regulators in stroma showed an age-specific effect. Except adiponectin, all other signaling of INSR and of related members studied was lower in the stroma of 10- and 21-mo-old animals compared to that of fetal ages. Whether age-specific decline in expression patterns of these mediators is a function of the endocrine milieu that prevails in postpubertal and adult animals remains to be ascertained.

Impact of Prenatal Steroids Excess

The effects of prenatal T and DHT treatment were restricted to two of the six mediators studied, namely PPARG and adiponectin. The selective increase in PPARG immunostaining in the ovaries of Fetal Day 90 and 140 prenatal T-treated fetuses accompanies our previously reported increase in AR expression seen at these ages in these very same animals [12]. PPARG may, therefore, be one of the early mediators in the developmental programming of adult ovarian dysfunction by prenatal T excess. The increased PPARG expression in the ovary of prenatal T-treated sheep appears to be mediated by androgenic actions of T because the nonaromatizable androgen, DHT, also increased PPARG immunostaining. Considering that agonists of PPARG reduce basal and LH-stimulated thecal androgen production [65] and limit granulosa cell estradiol production [65, 66], the PPARG up-regulation seen in response to T and DHT administration at fetal ages may function in a similar manner to limit androgen production at the stromal level.

The decrease in adiponectin expression in the granulosa cells of 10- and 21-mo-old prenatal T-treated females, on the other hand, would compromise follicular environment and prevent follicular maturation to the preovulatory state, thus contributing to the development of multifollicular ovaries in prenatal T-treated females [8–11]. The decreased adiponectin levels in prenatal T-treated females may be a function of altered steroid receptor balance. Granulosa cells of antral follicles in prenatal T-treated females manifest increased expression of AR and ESR1 and reduced expression of ESR2 [12]. Absence of similar changes in prenatal DHT-treated females suggests that the reduced granulosa cell adiponectin expression may be facilitated via estrogenic programming. Paradoxically, the regulation at the stromal level was similar for both prenatal T and DHT-treated animals suggestive of differential effects of androgenic and estrogenic programming at the various ovarian compartments.

Translational Significance

The findings from this study are likely to be of translational relevance to the ovarian phenotype of women with PCOS, whose characteristics the prenatal T-treated females recapitu-

late. While ovarian measures of adiponectin levels are not available, circulating levels of adiponectin are reduced in women with PCOS [24, 67]. Genomic studies also implicate hypoadiponectinemia in the etiology of PCOS [68]. Hypoadiponectinemia is also evident in other insulin-resistance states [69, 70]. As such, the reduced adiponectin levels in the ovaries of prenatal T-treated sheep are consistent with these animals being insulin resistant [13, 71]. It has been proposed that decreased adiponectin levels in PCOS women may be a contributing factor in the increased androgen production from theca cells [62].

In conclusion, we have demonstrated that key members of the insulin signaling cascade and related metabolic proteins are expressed at different stages of ovarian follicular development in the sheep, with PPARG expression increasing with prenatal T excess during fetal life and adiponectin decreasing during adult life. The findings are supportive of a role for PPARG in the programming of ovarian disruptions that includes a reduction in adiponectin levels in antral follicles and consequent failure of follicles to progress to preovulatory state.

REFERENCES

1. Webb R, Campbell BK. Development of the dominant follicle: mechanisms of selection and maintenance of oocyte quality. Soc Reprod Fertil Suppl 2007; 64:141–163.
2. Padmanabhan V, Manikkam M, Recabarren S, Foster D. Prenatal testosterone excess programs reproductive and metabolic dysfunction in the female. Mol Cell Endocrinol 2006; 246:165–174.
3. Abbott DH, Padmanabhan V, Dumesic DA. Contributions of androgen and estrogen to fetal programming of ovarian dysfunction. Reprod Biol Endocrinol 2006; 4:17.
4. Dumesic DA, Abbott DH, Padmanabhan V. Polycystic ovary syndrome and its developmental origins. Rev Endocr Metab Disord 2007; 8:127–141.
5. Dunaif A. Insulin resistance and the polycystic ovary syndrome: mechanism and implications for pathogenesis. Endocr Rev 1997; 18:774–800.
6. Rosenfield RL. Current concepts of polycystic ovary syndrome. Baillieres Clin Obstet Gynaecol 1997; 11:307–333.
7. Franks S, McCarthy MI, Hardy K. Development of polycystic ovary syndrome: involvement of genetic and environmental factors. Int J Androl 2006; 29:278–285.
8. West C, Foster DL, Evans NP, Robinson J, Padmanabhan V. Intra-follicular activin availability is altered in prenatally-androgenized lambs. Mol Cell Endocrinol 2001; 185:51–59.
9. Smith P, Steckler TL, Veiga-Lopez A, Padmanabhan V. Developmental programming: differential effects of prenatal testosterone and dihydrotestosterone on follicular recruitment, depletion of follicular reserve, and ovarian morphology in sheep. Biol Reprod 2009; 80:726–736.
10. Manikkam M, Steckler TL, Welch KB, Inskeep EK, Padmanabhan V. Fetal programming: prenatal testosterone treatment leads to follicular persistence/luteal defects; partial restoration of ovarian function by cyclic progesterone treatment. Endocrinology 2006; 147:1997–2007.
11. Steckler T, Manikkam M, Inskeep EK, Padmanabhan V. Developmental programming: follicular persistence in prenatal testosterone-treated sheep is not programmed by androgenic actions of testosterone. Endocrinology 2007; 148:3532–3540.
12. Ortega HH, Salvetti NR, Padmanabhan V. Developmental programming: prenatal androgen excess disrupts ovarian steroid receptor balance. Reproduction 2009; 137:865–877.
13. Recabarren SE, Padmanabhan V, Codner E, Lobos A, Durán C, Vidal M,

Foster DL, Sirpetermann T. Postnatal developmental consequences of altered insulin sensitivity in female sheep treated prenatally with testosterone. Am J Physiol Endocrinol Metab 2005; 289:801–806.

14. Willis D, Mason H, Gilling-Smith C, Franks S. Modulation by insulin of follicle-stimulating hormone and luteinizing hormone actions in human granulosa cells of normal and polycystic ovaries. J Clin Endocrinol Metab 1996; 81:302–309.

15. Adashi EY, Resnick CE, Payne DW, Rosenfeld RG, Matsumoto T, Hunter MK, Gargosky SE, Zhou J, Bondy CA. The mouse intraovarian insulin-like growth factor I system: departures from the rat paradigm. Endocrinology 1997; 138:3881–3890.

16. Poretsky L, Cataldo NA, Rosenwaks Z, Giudice LC. The insulin-related ovarian regulatory system in health and disease. Endocr Rev 1999; 20: 535–582.

17. Neganova I, Al-Qassab H, Heffron H, Selman C, Choudhury AI, Lingard SJ, Diakonov I, Patterson M, Ghatei M, Bloom SR, Franks S, Huhtaniemi I, et al. Role of central nervous system and ovarian insulin receptor substrate 2 signaling in female reproductive function in the mouse. Biol Reprod 2007; 76:1045–1053.

18. Ledoux S, Campos DB, Lopes FL, Dobias-Goff M, Palin MF, Murphy BD. Adiponectin induces periovulatory changes in ovarian follicular cells. Endocrinology 2006; 147:5178–5186.

19. Seto-Young D, Avtanski D, Strizhevsky M, Parikh G, Patel P, Kaplun J, Holcomb K, Rosenwaks Z, Poretsky L. Interactions among peroxisome proliferator activated receptor-gamma, insulin signaling pathways, and steroidogenic acute regulatory protein in human ovarian cells. J Clin Endocrinol Metab 2007; 92:2232–2239.

20. Baba T, Endo T, Sata F, Honnma H, Kitajima Y, Hayashi T, Manase K, Kanaya M, Yamada H, Minakami H, Kishi R, Saito T. Polycystic ovary syndrome is associated with genetic polymorphism in the insulin signaling gene IRS-1 but not ENPP1 in a Japanese population. Life Sci 2007; 81: 850–854.

21. Kayampilly PP, Menon KM. Dihydrotestosterone inhibits insulin-stimulated cyclin D2 messenger ribonucleic acid expression in rat ovarian granulosa cells by reducing the phosphorylation of insulin receptor substrate-1. Endocrinology 2006; 147:464–471.

22. Yaba A, Bianchi V, Borini A, Johnson J. A putative mitotic checkpoint dependent on mTOR function controls cell proliferation and survival in ovarian granulosa cells. Reprod Sci 2008; 15:128–138.

23. Dunaif A, Thomas A. Current concepts in the polycystic ovary syndrome. Annu Rev Med 2001; 52:401–419.

24. Ardawi MS, Rouzi AA. Plasma adiponectin and insulin resistance in women with polycystic ovary syndrome. Fertil Steril 2005; 83:1708–1716.

25. Barber TM, McCarthy MI, Wass JA, Franks S. Obesity and polycystic ovary syndrome. Clin Endocrinol (Oxf) 2006; 65:137–145.

26. Qu J, Wang Y, Wu X, Gao L, Hou L, Erkkola R. Insulin resistance directly contributes to androgenic potential within ovarian theca cells. Fertil Steril 2009; 91:1990–1997.

27. Burks DJ, Font de MJ, Schubert M, Withers DJ, Myers MG, Towery HH, Altamuro SL, Flint CL, White MF. IRS-2 pathways integrate female reproduction and energy homeostasis. Nature 2000; 407:377–382.

28. Kim J, Sato M, Li Q, Lydon JP, Demayo FJ, Bagchi IC, Bagchi MK. Peroxisome proliferator-activated receptor gamma is a target of progesterone regulation in the preovulatory follicles and controls ovulation in mice. Mol Cell Biol 2008; 28:1770–1782.

29. Cui Y, Miyoshi K, Claudio E, Siebenlist UK, Gonzalez FJ, Flaws J, Wagner KU, Hennighausen L. Loss of the peroxisome proliferation-activated receptor gamma (PPARgamma) does not affect mammary development and propensity for tumor formation but leads to reduced fertility. J Biol Chem 2002; 277:17830–17835.

30. Saltiel AR, Kahn CR. Insulin signalling and the regulation of glucose and lipid metabolism. Nature 2001; 414:799–806.

31. Lizcano JM, Alessi DR. The insulin signalling pathway. Curr Biol 2002; 12:R236–R238.

32. Alam H, Weck J, Maizels E, Park Y, Lee EJ, Ashcroft M, Hunzicker-Dunn M. Role of the phosphatidylinositol-3-kinase and extracellular regulated kinase pathways in the induction of hypoxia-inducible factor (HIF)-1 activity and the HIF-1 target vascular endothelial growth factor in ovarian granulosa cells in response to follicle-stimulating hormone. Endocrinology 2009; 150:915–928.

33. Carvalho CR, Carvalheira JB, Lima MH, Zimmerman SF, Caperuto LC, Amanso A, Gasparetti AL, Meneghetti V, Zimmerman LF, Velloso LA, Saad MJ. Novel signal transduction pathway for luteinizing hormone and its interaction with insulin: activation of Janus kinase/signal transducer and activator of transcription and phosphoinositol 3-kinase/Akt pathways. Endocrinology 2003; 144:638–647.

34. Lima MH, Souza LC, Caperuto LC, Bevilacqua E, Gasparetti AL, Zanuto

R, Saad MJ, Carvalho CR. Up-regulation of the phosphatidylinositol 3-kinase/protein kinase B pathway in the ovary of rats by chronic treatment with hCG and insulin. J Endocrinol 2006; 190:451–459.

35. Yen HW, Jakimiuk AJ, Munir I, Magoffin DA. Selective alterations in insulin receptor substrates-1, -2 and -4 in theca but not granulosa cells from polycystic ovaries. Mol Hum Reprod 2004; 10:473–479.

36. Diamanti-Kandarakis E, Argyrakopoulou G, Economou F, Kandaraki E, Koutsilieris M. Defects in insulin signaling pathways in ovarian steroidogenesis and other tissues in polycystic ovary syndrome (PCOS). J Steroid Biochem Mol Biol 2008; 109:242–246.

37. Samoto T, Maruo T, Ladines-Llave CA, Matsuo H, Deguchi J, Barnea ER, Mochizuki M. Insulin receptor expression in follicular and stromal compartments of the human ovary over the course of follicular growth, regression and atresia. Endocr J 1993; 40:715–726.

38. Willis D, Franks S. Insulin action in human granulosa cells from normal and polycystic ovaries is mediated by the insulin receptor and not the type-I insulin-like growth factor receptor. J Clin Endocrinol Metab 1995; 80: 3788–3790.

39. Phy JL, Conover CA, Abbott DH, Zschunke MA, Walker DL, Session DR, Tummon IS, Thornhill AR, Lesnick TG, Dumesic DA. Insulin and messenger ribonucleic acid expression of insulin receptor isoforms in ovarian follicles from nonhirsute ovulatory women and polycystic ovary syndrome patients. J Clin Endocrinol Metab 2004; 89:3561–3566.

40. Seli E, Duleba AJ. Treatment of PCOS with metformin and other insulin-sensitizing agents. Curr Diab Rep 2004; 4:69–75.

41. Stout DL, Fugate SE. Thiazolidinediones for treatment of polycystic ovary syndrome. Pharmacotherapy 2005; 25:244–252.

42. Elkind-Hirsch KE. Thiazolidinediones for the therapeutic management of polycystic ovary syndrome: impact on metabolic and reproductive abnormalities. Treat Endocrinol 2006; 5:171–187.

43. Steckler TL, Herkimer C, Dumesic DA, Padmanabhan V. Developmental programming: excess weight gain amplifies the effects of prenatal testosterone excess on reproductive cyclicity—implication for polycystic ovary syndrome. Endocrinology 2009; 150:1456–1465.

44. Chabrolle C, Tosca L, Dupont J. Regulation of adiponectin and its receptors in rat ovary by human chorionic gonadotrophin treatment and potential involvement of adiponectin in granulosa cell steroidogenesis. Reproduction 2007; 133:719–731.

45. Sieminska L, Marek B, Kos-Kudla B, Niedziolka D, Kajdaniuk D, Nowak M, Glogowska-Szelag J. Serum adiponectin in women with polycystic ovarian syndrome and its relation to clinical, metabolic and endocrine parameters. J Endocrinol Invest 2004; 27:528–534.

46. Panidis D, Farmakiotis D, Rousso D, Koliakos G, Kaltsas T, Krassas G. Decrease in adiponectin levels in women with polycystic ovary syndrome after an oral glucose tolerance test. Fertil Steril 2005; 83:232–234.

47. Sepilian V, Nagamani M. Adiponectin levels in women with polycystic ovary syndrome and severe insulin resistance. J Soc Gynecol Investig 2005; 12:129–134.

48. Escobar-Morreale HF, Villuendas G, Botella-Carretero JI, Alvarez-Blasco F, Sanchon R, Luque-Ramirez M, San Millan JL. Adiponectin and resistin in PCOS: a clinical, biochemical and molecular genetic study. Hum Reprod 2006; 21:2257–2265.

49. Aroda V, Ciaraldi TP, Chang SA, Dahan MH, Chang RJ, Henry RR. Circulating and cellular adiponectin in polycystic ovary syndrome: relationship to glucose tolerance and insulin action. Fertil Steril 2008; 89:1200–1208.

50. Manikkam M, Crespi EJ, Doop DD, Herkimer C, Lee JS, Yu S, Brown MB, Foster DL, Padmanabhan V. Fetal programming: prenatal testosterone excess leads to fetal growth retardation and postnatal catch-up growth in sheep. Endocrinology 2004; 145:790–798.

51. Steckler TL, Lee JS, Ye W, Inskeep EK, Padmanabhan V. Developmental programming: exogenous gonadotropin treatment rescues ovulatory function but does not completely normalize ovarian function in sheep treated prenatally with testosterone. Biol Reprod 2008; 79:686–695.

52. Zhu LJ, Hardy MP, Inigo IV, Huhtaniemi I, Bardin CW, Moo-Young AJ. Effects of androgen on androgen receptor expression in rat testicular and epididymal cells: a quantitative immunohistochemical study. Biol Reprod 2000; 63:368–376.

53. Lejeune M, Jaen J, Pons L, Lopez C, Salvado MT, Bosch R, Garcia M, Escriva P, Baucells J, Cugat X, Alvaro T. Quantification of diverse subcellular immunohistochemical markers with clinicobiological relevancies: validation of a new computer-assisted image analysis procedure. J Anat 2008; 212:868–878.

54. Pham NA, Morrison A, Schwock J, Aviel-Ronen S, Iakovlev V, Tsao MS, Ho J, Hedley DW. Quantitative image analysis of immunohistochemical stains using a CMYK color model. Diagn Pathol 2007; 2:8.

55. Theodosiou Z, Kasampalidis IN, Livanos G, Zervakis M, Pitas I, Lyroudia

K. Automated analysis of FISH and immunohistochemistry images: a review. Cytometry A 2007; 71:439–450.

56. Peretti-Renucci R, Feuerstein C, Manier M, Lorimier P, Savasta M, Thibault J, Mons N, Geffard M. Quantitative image analysis with densitometry for immunohistochemistry and autoradiography of receptor binding sites—methodological considerations. J Neurosci Res 1991; 28: 583–600.

57. Alam H, Maizels ET, Park Y, Ghaey S, Feiger ZJ, Chandel NS, Hunzicker-Dunn M. Follicle-stimulating hormone activation of hypoxia-inducible factor-1 by the phosphatidylinositol 3-kinase/AKT/Ras homolog enriched in brain (Rheb)/mammalian target of rapamycin (mTOR) pathway is necessary for induction of select protein markers of follicular differentiation. J Biol Chem 2004; 279:19431–19440.

58. Kowalewski MP, Dyson MT, Manna PR, Stocco DM. Involvement of peroxisome proliferator-activated receptor gamma in gonadal steroido-genesis and steroidogenic acute regulatory protein expression. Reprod Fertil Dev 2009; 21:909–922.

59. Lord E, Ledoux S, Murphy BD, Beaudry D, Palin MF. Expression of adiponectin and its receptors in swine. J Anim Sci 2005; 83:565–578.

60. Yamauchi T, Kamon J, Waki H, Murakami K, Motojima K, Komeda K, Ide T, Kubota N, Terauchi Y, Tobe K, Miki H, Tsuchida A, et al. The mechanisms by which both heterozygous peroxisome proliferator-activated receptor gamma (PPARgamma) deficiency and PPARgamma agonist improve insulin resistance. J Biol Chem 2001; 276:41245–41254.

61. Nawrocki AR, Rajala MW, Tomas E, Pajvani UB, Saha AK, Trumbauer ME, Pang Z, Chen AS, Ruderman NB, Chen H, Rossetti L, Scherer PE. Mice lacking adiponectin show decreased hepatic insulin sensitivity and reduced responsiveness to peroxisome proliferator-activated receptor gamma agonists. J Biol Chem 2006; 281:2654–2660.

62. Lagaly DV, Aad PY, Grado-Ahuir JA, Hulsey LB, Spicer LJ. Role of adiponectin in regulating ovarian theca and granulosa cell function. Mol Cell Endocrinol 2008; 284:38–45.

63. Ma K, Cabrero A, Saha PK, Kojima H, Li L, Chang BH, Paul A, Chan L. Increased beta-oxidation but no insulin resistance or glucose intolerance in mice lacking adiponectin. J Biol Chem 2002; 277:34658–34661.

64. Yamauchi T, Nio Y, Maki T, Kobayashi M, Takazawa T, Iwabu M, Okada-Iwabu M, Kawamoto S, Kubota N, Kubota T, Ito Y, Kamon J, et al. Targeted disruption of AdipoR1 and AdipoR2 causes abrogation of adiponectin binding and metabolic actions. Nat Med 2007; 13:332–339.

65. Schoppee PD, Garmey JC, Veldhuis JD. Putative activation of the peroxisome proliferator-activated receptor gamma impairs androgen and enhances progesterone biosynthesis in primary cultures of porcine theca cells. Biol Reprod 2002; 66:190–198.

66. Komar CM, Curry TE Jr. Localization and expression of messenger RNAs for the peroxisome proliferator-activated receptors in ovarian tissue from naturally cycling and pseudopregnant rats. Biol Reprod 2002; 66:1531–1539.

67. Panidis D, Kourtis A, Farmakiotis D, Mouslech T, Rousso D, Koliakos G. Serum adiponectin levels in women with polycystic ovary syndrome. Hum Reprod 2003; 18:1790–1796.

68. Escobar-Morreale HF, Luque-Ramirez M, San Millan JL. The molecular-genetic basis of functional hyperandrogenism and the polycystic ovary syndrome. Endocr Rev 2005; 26:251–282.

69. Weyer C, Funahashi T, Tanaka S, Hotta K, Matsuzawa Y, Pratley RE, Tataranni PA. Hypoadiponectinemia in obesity and type 2 diabetes: close association with insulin resistance and hyperinsulinemia. J Clin Endocrinol Metab 2001; 86:1930–1935.

70. Ranheim T, Haugen F, Staff AC, Braekke K, Harsem NK, Drevon CA. Adiponectin is reduced in gestational diabetes mellitus in normal weight women. Acta Obstet Gynecol Scand 2004; 83:341–347.

71. Padmanabhan V, Veiga-Lopez A, Abbott D, Recabarren S, Herkimer C. Developmental programming: impact of prenatal testosterone excess and postnatal weight gain on insulin sensitivity index and transfer of traits to offspring of overweight females. Endocrinology 2009; 151:595–605.